J|A|C|S ARTICLES

Published on Web 03/06/2009

Active-Site Motions and Polarity Enhance Catalytic Turnover of Hydrated Subtilisin Dissolved in Organic Solvents

Elton P. Hudson,[†] Ross K. Eppler,[†] Julianne M. Beaudoin,[†] Jonathan S. Dordick,[‡] Jeffrey A. Reimer,[†] and Douglas S. Clark*[,†]

Department of Chemical Engineering, University of California, Berkeley, California 94720, and Department of Chemical and Biological Engineering, Rensselaer Polytechnic Institute, Troy, New York 12180

Received September 3, 2008; E-mail: clark@berkeley.edu

Abstract: The enzyme subtilisin Carlsberg was surfactant-solubilized into two organic solvents, isooctane and tetrahydrofuran, and hydrated through stepwise changes in the thermodynamic water activity, a_w. The apparent turnover number k_{cat}^{app} in these systems ranged from 0.2 to 80 s^{-1} and increased 11-fold in isooctane and up to 50-fold in tetrahydrofuran with increasing a_w. ^{19}F NMR relaxation experiments employing an active-site inhibitor were used to assess the dependence of active-site motions on a_w. The rates of NMR-derived fast ($k > 10^7$ s^{-1}) and slow ($k < 10^4$ s^{-1}) active-site motions increased in both solvents upon hydration, but only the slow motions correlated with k_{cat}. The ^{19}F chemical shift was a sensitive probe of the local electronic environment and provided an empirical measure of the active-site dielectric constant ε_{as}, which increased with hydration to $\varepsilon_{as} \approx 13$ in each solvent. In both solvents, the transition state free energy data and ε_{as} followed Kirkwood's model for the continuum solvation of a dipole, indicating that water also enhanced catalysis by altering the active-site's electronic environment and increasing its polarity to better stabilize the transition state. These results reveal that favorable dynamic and electrostatic effects both contribute to accelerated catalysis by solubilized subtilisin Carlsberg upon hydration in organic solvents.

Introduction

The relationship between protein motion and function has been extensively analyzed through theoretical and experimental avenues. From this large body of work, it is apparent that motions occurring on several timescales are related to, and may even be required for, catalysis by many enzymes.[1−4] Nonaqueous biocatalysis is an arena where dynamics−function relationships can be further explored in a unique way. The restriction of protein motions in anhydrous or nearly anhydrous organic media is thought to be a significant factor in the generally poor catalytic performance of enzymes in nonaqueous solvents,[5,6] and the addition of water has been shown to increase subnanosecond motions in solvent-suspended enzyme powders while increasing catalytic activity.[7,8] In addition to this role, in the particular case of subtilisin, there is evidence that water increases the dielectric at the enzyme's active site in anhydrous solvents,[9] possibly affecting electronic interactions that are known to be critical for transition state stabilization.[10−12] Hydration of enzymes in organic solvents thus allows for exploration of the roles of both protein dynamics and local electrostatics in promoting catalysis.

In the present work, subtilisin Carlsberg (SC) was ion-paired with the surfactant Aerosol OT (AOT) and extracted into isooctane, then redissolved in two organic solvents, isooctane and tetrahydrofuran (THF). The enzyme was hydrated through changes in the thermodynamic water activity a_w, an indirect yet accurate descriptor of the amount of water bound to the enzyme, with $a_w > 0.9$ typically required for monolayer water coverage.[13−16] Information on active-site motions and structure, and the local electronic environment, was obtained from the ^{19}F NMR resonance of a covalently bound aromatic active-site inhibitor, 4-fluorobenzene sulfonyl fluoride (4FBSF), which irreversibly acylates the active-site Ser221 residue.

[†] University of California.
[‡] Rensselaer Polytechnic Institute.

(1) Henzler-Wildman, K. A.; Lei, M.; Thai, V.; Kerns, S. J.; Karplus, M.; Kern, D. *Nature* **2007**, *450*, 913–6.
(2) Frauenfelder, H.; Sligar, S. G.; Wolynes, P. G. *Science* **1991**, *254*, 1598–603.
(3) Warshel, A. *Proc. Natl. Acad. Sci. U.S.A.* **1984**, *81*, 444–8.
(4) Sola, R. J.; Griebenow, K. *FEBS J.* **2006**, *273*, 5303–19.
(5) Clark, D. S. *Philos. Trans. R. Soc. London, Ser. B* **2004**, *359*, 1323–1328.
(6) Schmitke, J. L.; Westcott, C. R.; Klibanov, A. M. *J. Am. Chem. Soc.* **1996**, *118*, 3360–3365.
(7) Partridge, J.; Dennison, P. R.; Moore, B. D.; Halling, P. J. *Biochim. Biophys. Acta* **1998**, *1386*, 79–89.
(8) Kurkal, V.; Daniel, R. M.; Finney, J. L.; Tehei, M.; Dunn, R. V.; Smith, J. C. *Biophys. J.* **2005**, *89*, 1282–7.
(9) Affleck, R.; Xu, Z. F.; Suzawa, V.; Focht, K.; Clark, D. S.; Dordick, J. S. *Proc. Natl. Acad. Sci. U.S.A.* **1992**, *89*, 1100–4.
(10) Warshel, A.; Naray-Szabo, G.; Sussman, F.; Hwang, J. K. *Biochemistry* **1989**, *28*, 3629–37.
(11) Jackson, S. E.; Fersht, A. R. *Biochemistry* **1993**, *32*, 13909–16.
(12) Carter, P.; Wells, J. A. *Proteins* **1990**, *7*, 335–42.
(13) Halling, P. J. *Biotechnol. Tech.* **1992**, *6*, 271–276.
(14) Halling, P. J. *Enzyme Microb. Technol.* **1994**, *16*, 178–207.
(15) Parker, M. C.; Moore, B. D.; Blacker, A. J. *Biotechnol. Bioeng.* **1995**, *46*, 452–458.
(16) McMinn, J. H.; Sowa, M. J.; Charnick, S. B.; Paulaitis, M. E. *Biopolymers* **1993**, *33*, 1213–24.

10.1021/ja806996q CCC: $40.75

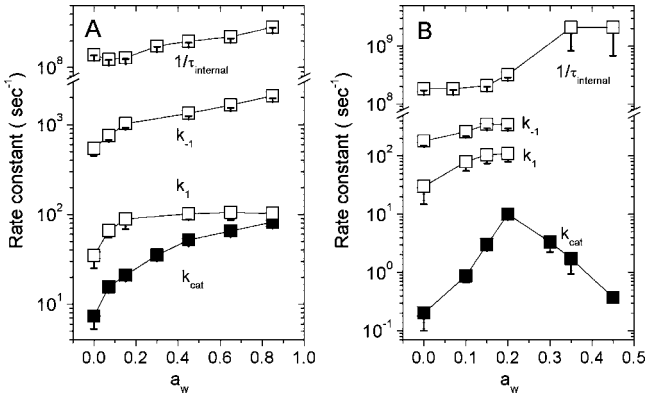

Figure 1. Catalytic and motional rate constants at the active site of ion-paired subtilisin Carlsberg (SC) in isooctane (A) and THF (B). The rate constants were quantified using a variety of ^{19}F NMR experiments with 4FBS-SC at 25 °C as described in Data Analysis. Apparent turnover k_{cat}^{app} is for transesterification of N-Ac-Phe-ethyl ester (APEE) with 0.85 M 1-PrOH at 30 °C. Rapid precipitation of inactive biocatalyst in THF at $a_w > 0.5$ prevented experiments at higher a_w in this solvent.

Internal aromatic rings are useful NMR probes for protein conformational mobility, as their rotation frequently requires reorganization of the protein backbone or sidechains. Aromatic residues in aqueous and organic-suspended proteins exhibit a broad range of rate constants for rotation or flipping, from 10^2 $s^{-1} < k < 10^8$ s^{-1} as determined primarily through NMR line-shape analysis.[17,18] Herein, we fit NMR relaxation data for 4FBS-SC to motional models to discriminate between nano-second active-site fluctuations that allow for internal ring rotation about the C−F axis ($1/\tau_{internal} = k > 10^8$ s^{-1}) and slower, more concerted motions (10 $s^{-1} < k < 10^3$ s^{-1}). A quantitative comparison of the rates of these processes to catalytic turnover as the enzyme is hydrated allows us to determine which of them may contribute to catalysis. The chemical shift of the 4FBS-SC resonance was used to calculate the active-site dielectric constant (ε_{as}). Knowledge of ε_{as} along with kinetic data describing the free energy of the transition state enabled us to examine how water facilitates catalysis through electrostatic interactions, and in particular its ability to solvate the enzyme's charged transition state, thereby lowering its free energy and increasing the rate of reaction.

Results and Discussion

Hydration Effects on Turnover. It has been shown previously that enzymes suspended in organic solvents exhibit increased reaction rates upon hydration.[9,19] Figure 1 shows the dependence of k_{cat}^{app} on a_w for organic-soluble SC, where k_{cat}^{app} was calculated using the concentration of accessible active sites in each preparation (see Experimental Section). Turnover increased with hydration 11-fold in isooctane, and 50-fold in THF, up to $a_w = 0.2$, although the biocatalyst was much less active in THF over the entire hydration range. The influence of a_w on SC catalysis in both isooctane and THF was primarily on catalytic turnover (Table 1), with only a minimal effect on K_m^{app}. However, in both isooctane and THF, there was a distinct increase in K_m^{app} as compared to aqueous buffer, with a more significant increase in THF. In contrast to what was observed in studies with suspended powders, in which the specific transesterification activity was constant for $a_w < 0.4$,[7] kinetic activation of the soluble enzyme did not increase sigmoidally with water activity. In the ion-paired form, neutralization of enzyme surface charges by surfactant and its counterion may result in altered water sorption characteristics, for example, directing water away from ionic groups[20] to regions of the protein where it may have a larger effect on catalysis.

The lower catalytic activity in THF is likely due to a decrease in the degree of tertiary structure in this solvent, as has been shown for ion-paired subtilisin BPN' by Wangikar et al.[21] Furthermore, the concentration of available active sites is lower in THF than in isooctane (see Experimental Section). The sharp decrease in k_{cat}^{app} observed at $a_w > 0.2$ in THF is likely due to a more complete unfolding of the enzyme, as evidenced by a sharp reduction of the internal rotational correlation time of 4-FBS (Figure 2), a decrease in the steady-state $\{^1H\}^{19}F$ nuclear Overhauser effect (NOE) of the 4FBS-SC resonance to the *ortho*-ring protons and the protein protons $H^{\alpha 2}$ Gly 128 and $H^{\alpha 1}$ Gly154, and loss of secondary structure as measured by circular dichroism (see Supporting Information). Importantly, the NOE of the 4FBS-SC resonance in isooctane approximated that in aqueous buffer and did not change as a function of a_w, which indicated that the solubilized enzyme in isooctane retained its native folded structure.

Active-Site Motions. Structural modeling of the 4FBS moiety at the active site (Figure 3) shows that the aromatic ring likely sits at the entrance to the specificity pocket of subtilisin, similar to the phenyl ring of the protease inhibitor phenylmethylsulfonyl fluoride.[22] When quantifying 4FBS motion in the active site, it is useful to assume a motional model. On the basis of the structure in Figure 3, we assumed that the ring motion is described by restricted rotation about the aromatic symmetry axis with a characteristic rotation time τ_{int}. The determination of τ_{int} from 4FBS-SC R_1 and R_2 relaxation data at multiple fields is depicted graphically in Figure 2A and described in Data Analysis. The calculated τ_{int} of <10 ns at all a_w values implies that the ring is not held rigidly but can rotate about the C−F bond axis with some active-site structural rearrangements. The rotation rate of the ring is thus used as a proxy for fast active-site motions.

Initial hydration to $a_w = 0.15$ produced no change in τ_{int} in either solvent (Figure 2). The insensitivity of τ_{int} is in contrast to the rise in k_{cat}^{app} over the same hydration range, indicating that fast active-site motions and turnover did not correlate (Figure 1). At $a_w > 0.2$, the rate of ring motion ($k = 1/\tau_{int}$) increased, steadily in isooctane and sharply in THF. In the latter case, τ_{int} decreased to 0.5 ns, consistent with unrestricted rotation and suggestive of an unstructured active site.[23]

Slower active-site motions, with rate constants ranging from 10 to 1000 s^{-1}, were quantified by fitting 4FBS-SC NMR relaxation dispersion data to the two-site chemical exchange equation, with the constants k_1 and k_{-1} describing the jumps between the two sites.[24] The types of active site motions detected by chemical exchange can range from small loop motions such

(17) Wagner, G.; DeMarco, A.; Wuthrich, K. *Biophys. Struct. Mech.* **1976**, *2*, 139–158.
(18) Burke, P. A.; Griffin, R. G.; Klibanov, A. M. *Biotechnol. Bioeng.* **1993**, *42*, 87–94.
(19) Zaks, A.; Klibanov, A. M. *J. Biol. Chem.* **1988**, *263*, 8017–21.
(20) Rupley, J. A.; Gratton, E.; Careri, G. *Trends Biochem. Sci.* **1983**, *8*, 18–22.
(21) Wangikar, P. P.; Michels, P. C.; Clark, D. S.; Dordick, J. S. *J. Am. Chem. Soc.* **1997**, *119*, 70–76.
(22) Gallagher, T.; Oliver, J.; Bott, R.; Betzel, C.; Gilliland, G. L. *Acta Crystallogr., Sect. D: Biol. Crystallogr.* **1996**, *52*, 1125–35.
(23) Cairi, M.; Gerig, J. T. *J. Am. Chem. Soc.* **1983**, *105*, 4793–4800.
(24) Palmer, A. G., III.; Kroenke, C. D.; Loria, J. P. *Methods Enzymol.* **2001**, *339*, 204–38.

Table 1. Kinetic Parameters for Extracted SC in Organic Solvents[a]

isooctane				THF			
a_w	k_{cat}^{app} (s^{-1})	K_M^{app} (mM)	k_{cat}/K_M (s^{-1} M^{-1})	a_w	k_{cat}^{app} (s^{-1})	K_M^{app} (mM)	k_{cat}/K_M (s^{-1} M^{-1})
0	7.3	31	235	0	0.2	109	1.8
0.07	15.5	29	530	0.07	0.9	124	7.0
0.11	21.1	35	600	0.11	2.9	165	18.1
0.35	35.0	36	970	0.2	10.0	205	49.2
0.45	52.1	44	1180	0.30	3.4	200	16.7
0.65	64.9	38	1710	0.35	1.74	180	9.6
0.85	81.8	41	1990	0.45	0.5	185	2.7
				aqueous[b]	500	12	42 000

[a] Transesterification of APEE with 0.85 M 1-PrOH at 30 °C. k_{cat} calculated using the active-site concentration as described in the Experimental Section. The k_{cat} determined in 0.85 M 1-PrOH was >90% of the fully saturated value in anhydrous THF and >95% in anhydrous isooctane. Similar comparisons were not made for other values of a_w; hence, the individual kinetic constants are labeled as apparent. [b] For hydrolysis of APEE at 30 °C.[51]

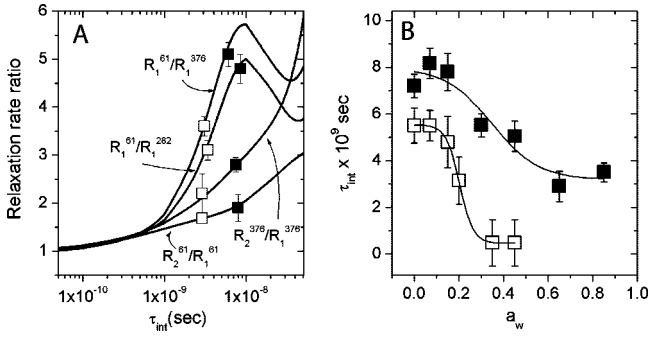

Figure 2. (A) Representative plots showing dependence of relaxation rate ratio on τ_{int} for 4FBS-SC in THF, $a_w = 0.2$ (□), and isooctane, $a_w = 0$ (■). The solid lines are theoretical relaxation ratios[38] at multiple static fields for a fixed global correlation time of 21 and 20 ns as described in Data Analysis. (B) τ_{int} in THF (□) and isooctane (■).

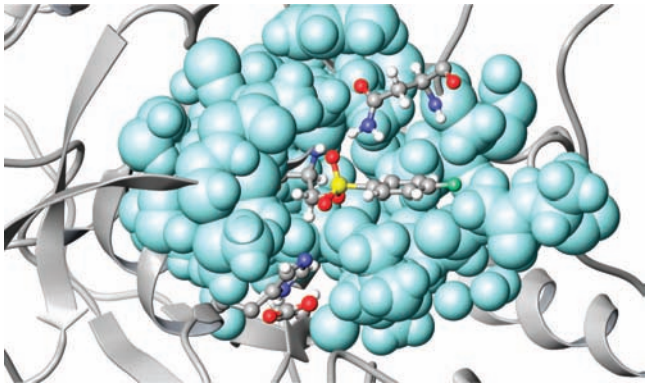

Figure 3. Molecular model of 4-FBS attached to Ser221 in the active site of SC. The fluorine nucleus is shown in green, and Asn155, Asp32, and His64 are shown in ball-and-stick format. Image created using Maestro as described in the Experimental Section.

as in the Met20 loop of dihydrofolate reductase,[25] to large (>1.5 nm) domain movements such as the lid closing of adenylate kinase.[1] However, subtilisin is not known to undergo any large structural changes during the reaction cycle.

Representative dispersion data and fits are shown in Figure 4A. To accurately determine k_1 and k_{-1} from the dispersion data, the temperature dependence of the dispersion effect was measured and is shown in Figure 4B (see Data Analysis). In contrast to ring rotation, the rate of these slow active-site motions increased 3-fold in the initial hydration regime ($0 < a_w < 0.2$) in both solvents (Figure 1, Table 2), suggesting a

(25) Schnell, J. R.; Dyson, H. J.; Wright, P. E. *Annu. Rev. Biophys. Biomol. Struct.* **2004**, *33*, 119–140.

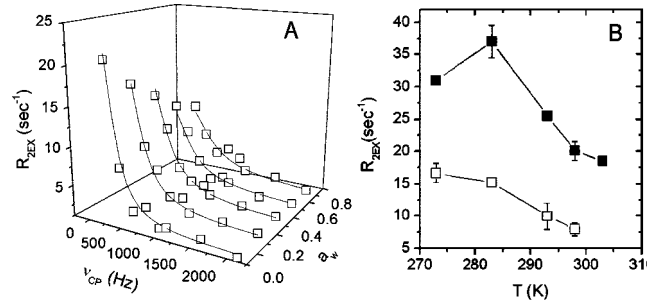

Figure 4. Chemical exchange contributions to ^{19}F transverse relaxation at 9.4 T (376 MHz). (A) Dependence on pulsing rate ν_{CP} is shown for 4FBS-SC in isooctane at 25 °C. The lines are fits to the two-site fast exchange equation (eq 2). (B) Temperature dependence of R_{EX} ($\nu_{CP} = 100$ s^{-1}) for $a_w = 0$ in isooctane (■), THF (□). A maximum R_{EX} was detected at 283 K in isooctane and surmised to occur at 273 K in THF, indicating the condition $k_{ex} = \Delta\omega$. This value of $\Delta\omega$ was fixed for calculations of k_1 and k_{-1} as described in Data Analysis. Lowering the sample temperature to 263 K in THF resulted in enzyme precipitation.

Table 2. ^{19}F Relaxation Dispersion Parameters for Extracted SC in Organic Solvents

isooctane[a]				THF[b]			
a_w	k_1	k_{-1}	p_B	a_w	k_1	k_{-1}	p_B
0	35 (9)	550 (100)	0.07	0	30 (15)	180 (30)	0.16
0.07	65 (11)	750 (90)	0.08	0.07	80 (25)	260 (40)	0.14
0.15	90 (20)	1020 (100)	0.07	0.15	105 (30)	350 (50)	0.15
0.45	100 (20)	1330 (85)	0.07	0.2	110 (30)[c]	345 (60)	0.08
0.65	105 (19)	1650 (110)	0.08	H_2O	n.d.	3150[d]	n.d.
0.85	100 (20)	2090 (100)	0.06	D_2O	n.d.	2900[d]	n.d.

[a] At 25 °C, using $\Delta\omega = 455$ Hz as described in the text. [b] At 25 °C, using $\Delta\omega = 190$ s^{-1}. [c] Exchange parameters were not calculated above $a_w > 0.2$ because $R_{2EX} \approx 0$ s^{-1} in these samples. [d] k_{ex}. Errors are indicated in parentheses.

correlation between the chemical exchange motion and turnover. In isooctane, k_1 was the same order of magnitude as k_{cat}^{app} over the whole hydration range; in THF, k_1, $k_{-1} \gg k_{cat}^{app}$, consistent with the notion that the enzyme samples distinct conformations on a timescale faster than turnover in this solvent.

Chemical exchange was not detected in THF at $a_w > 0.2$, which we suspect is due to a loss of structure around the active site. The disrupted active site could render the two conformers indistinguishable on the basis of chemical shift, resulting in a diminished dispersion effect (R_{EX} in eq 2). The reduction in R_{EX} could also be due to a sharp increase in k_1, k_{-1} at $a_w > 0.2$, or a change in the equilibrium distribution of protein conformations such that one becomes populated at less than 2%, which would make the dispersion effect undetectable.

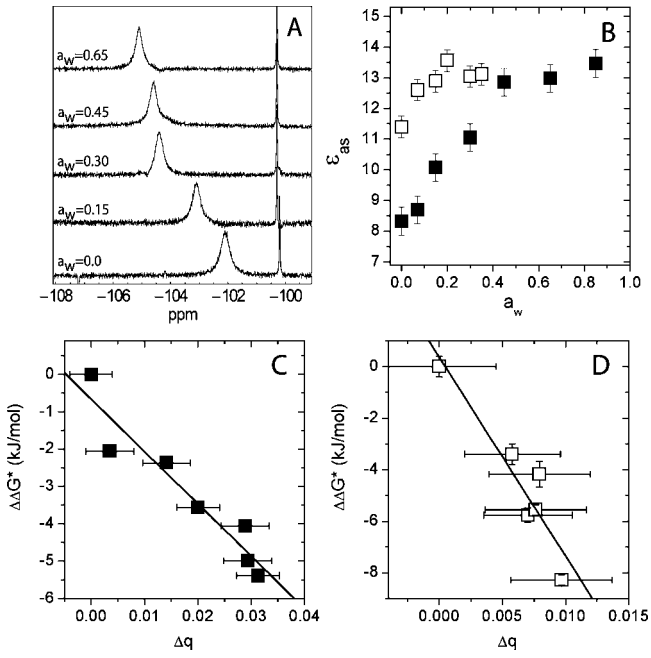

Figure 5. (A) ^{19}F NMR spectra of 4-FBS-SC in isooctane at 9.4 T referenced to $CFCl_3$. The broad peak in each spectrum corresponds to enzyme-bound 4-FBS, and the narrow peak to the aromatic fluorine of free 4-FBSF. (B) Effect of a_w on active-site dielectric constant in isooctane (■) and THF (□). Active-site dielectric constant was calculated from ^{19}F chemical shifts as described in Data Analysis. (C,D) Dependence of transition state free energy on dielectric factor as described in Data Analysis: isooctane (■), THF (□).

Active-Site Dielectric Constant. The sensitivity of fluorine nuclear shielding parameters and chemical shift to local electric fields has been exploited with some success to model complex electrical interactions in various proteins.[26−28] Here, we used an empirical correlation between the ^{19}F chemical shift and dielectric constant to probe the active-site electronic environment (eq 5 and Supporting Information). Representative 4FBS-subtilisin ^{19}F NMR spectra used for these calculations are shown in Figure 5A. The active-site dielectric constant ε_{as} as detected by the ^{19}F shift was sensitive to hydration in both solvents. In isooctane, it rose to 13.4 when the enzyme was hydrated to $a_w = 0.85$, whereas in THF it increased to 13.6 when $a_w = 0.2$ (Figure 5B). Based on the NMR chemical shift data, in isooctane there was no change in the bulk solvent dielectric constant over the entire hydration range, while in THF it rose from 7.7 to 8.1 at $a_w = 0.3$.

The increase in shift could be due to direct $H_2O-{}^{19}F$ interactions in the active site. An observed solvent deuterium isotope effect of 0.05 ppm for the 4FBS-SC resonance in ^{1}H THF/^{2}H THF indicates partial exposure of the fluorine nucleus to solvent. The observed shift was independent of the isotopic (^{2}H) composition of the water used in the extraction buffer and hydration. This is indicative of either no direct $H_2O-{}^{19}F$ contact or an isotope effect small enough, estimated to be $\Delta\delta_{H-D} <$ 0.04 ppm (16 Hz at 376 MHz), to be effectively masked by the line width of the 4FBS resonance. Direct $H_2O-{}^{19}F$ contact is not necessary to change the fluorine chemical shift, which is also sensitive to changes in ionization states or proximity of active-site residues,[29] as well as the orientation of the large helix dipole of Ser221.

In both solvents, the changes in ε_{as} with hydration correlated with catalytic turnover, suggesting stabilization of the polar transition state through a dielectric solvation effect. For solvation of a dipole in a spherical cavity, the continuum model of Kirkwood predicts a linear dependence of the dipole's free energy on the dielectric factor q (eqs 6−8) of the surrounding medium.[30] As applied to SC, the dipole is the enzyme's transition state, corresponding to a sphere with a diameter of approximately 0.9 nm, extending from the developing oxy-ion of APEE to the partially protonated ring of His64 and including any protein atoms within.[31] Free energies of activation are calculated from kinetic data, and the complex active-site electronic interactions from proximal protein residues and solvent are approximated as a continuum with a dielectric constant ε_{as}. A variant of this simple model was used previously to determine the dipole moment of the transition state of APEE-subtilisin suspended in organic solvents (31 Debye).[31]

From Figure 5C and D, the relationship between $\Delta\Delta G^*$ and Δq was linear in both solvents, suggesting that the increase in turnover with hydration can be described in terms of a dielectric solvation effect on the transition state. The magnitude of the slope was larger in the plot for THF, indicating a greater sensitivity of the reaction to the active-site dielectric constant. From eq 8, this greater dependence could be due to a change in transition state properties in THF[32] such as a larger dipole moment.

Conclusions

Changes in active-site motion and polarity as SC was hydrated in two organic solvents show that water promotes protein motion on both fast ($k = 1/\tau_{internal} > 10^8$ s^{-1}) and slow ($k < 10^4$ s^{-1}) timescales; however, only the slower chemical exchange processes with rates closer to catalytic turnover (k_{cat}^{app}) correlated with catalysis. However, a functional link between protein dynamics and turnover was not necessary to explain the increase in turnover with hydration, as the data fit the Kirkwood model for dielectric solvation of the transition state in each solvent. This Article thus illustrates the importance of considering active-site electrostatics as well as protein motion when developing relationships between protein physicochemical properties and catalytic activity, especially in organic solvents.

Data Analysis

Fast Active-Site Motions: Determination of τ_{int}. Fast motions at the active site were measured through the correlation time τ_{int} of the 4FBS ring while bound to Ser221. Rotation of the ring requires small structural perturbations in the active site (Figure 3) and is separate from the overall protein tumbling described by τ_c. Calculation of τ_{int} from ^{19}F NMR relaxation data followed the method and equations outlined by Hull and Sykes[33,34] and used extensively by Gerig et al.[35,36] The ring is

(26) Pearson, J. G.; Oldfield, E.; Lee, F. S.; Warshel, A. *J. Am. Chem. Soc.* **1993**, *115*, 6851–6862.
(27) Lau, E.; Gerig, J. *J. Am. Chem. Soc.* **2000**, *122*, 4408–4417.
(28) Kubasik, M. A.; Daly, E.; Blom, A. *ChemBioChem* **2006**, *7*, 1056–61.
(29) Gerig, J. T. *Prog. Nucl. Magn. Reson.* **1994**, *26*, 293–370.
(30) Kirkwood, J. G. *J. Chem. Phys.* **1934**, *2*, 351–361.
(31) Michels, P. C.; Dordick, J. S.; Clark, D. S. *J. Am. Chem. Soc.* **1997**, *119*, 9331–9335.
(32) Serdakowski, A. L.; Munir, I. Z.; Dordick, J. S. *J. Am. Chem. Soc.* **2006**, *128*, 14272–3.
(33) Hull, W. E.; Sykes, B. D. *J. Mol. Biol.* **1975**, *98*, 121–53.
(34) Hull, W. E.; Sykes, B. D. *Biochemistry* **1974**, *13*, 3431–7.
(35) Gerig, J. T.; Halley, B. A.; Ortiz, C. E. *J. Am. Chem. Soc.* **1977**, *99*, 6219–26.

assumed to rotate about its symmetry axis in the active site of the enzyme, and the $^{19}F-^{1}H$ dipolar interaction and ^{19}F chemical shift anisotropy are considered as relaxation mechanisms. This is an alternative to the popular "model-free" developed by Lipari and Szabo,[37] as it does not assume $\tau_{int} \ll \tau_c$.

The solid lines in Figure 2A are theoretical dependencies of four NMR relaxation ratios on τ_{int}, calculated using physical inputs described below. Four experimentally determined R_1/R_1 and R_1/R_2 inputs were used to calculate τ_{int} for each enzyme preparation, according to Hull and Sykes.[33,34] Figure 2A compares the calculated τ_{int} values for two enzyme preparations to the theoretical R ratio curves and illustrates that each τ_{int} value is nearly constant across all four curves. The mean values of these τ_{int} values for each enzyme preparation are reported in Figure 2B, along with their standard deviations.

For the dipole relaxation mechanism of the ^{19}F nucleus, *ortho*-ring protons and two proximal enzyme protons, $H^{\alpha 2}$ Gly 128 and $H^{\alpha 1}$ Gly 154, were explicitly considered. The $^{1}H-^{19}F$ internuclear distances of these protons and their orientations relative to the diffusion axis (parallel to the C−F bond) were taken from the minimized 4FBS-SC structure. Full coordinates of this structure are given as a link in the Supporting Information. For the chemical shift anisotropy mechanism, the z-component of the chemical shift tensor in its principal axis system (perpendicular to the ring) and the asymmetry of the tensor were taken from fluorobenzene data to be −58.2 ppm and 1.27, respectively.[33] The alignment of the chemical shift tensor to the diffusion axis was taken to be 90°, 90°, and 0° as calculated for *p*-fluorophenylalanine.[33] The global tumbling time τ_c was determined with light scattering to be 21 ns in octane and 20 ns in THF.

The dominant source of relaxation for the ^{19}F nucleus of 4FBS is the dipolar interaction with *ortho*-ring protons, and the internuclear distances and angles involved should not change with solvent or hydration. Furthermore, τ_{int} values calculated from relaxation rate ratios are sensitive to the distances of nearby (<0.40 nm) protein protons. These distances were treated as fixed experimental inputs in our calculations, but they could conceivably vary with the solvent and/or hydration level of the protein. However, comparing τ_{int} values calculated with and without the presence of protein protons, which represents an unrealistic extreme, revealed that the maximum effect on τ_{int} was less than 30% in the worst case.

Slow Active-Site Motions: Chemical Exchange. Slower motions at the active site were detected and quantified by fitting NMR relaxation dispersion data to a two-site fast chemical exchange model.[39] Relaxation dispersion has been used extensively to quantify the rates of interconversion between protein conformations, such as dihydrofolate reductase sampling open and occluded states during its catalytic cycle.[40] As applied to the 4FBS-SC, the exchange process represents more concerted motions than the fast fluctuations that allow the ring rotation described by τ_{int}.

The contribution from chemical exchange to R_2 of the 4FBS-SC resonance is R_{EX} (eq 1). The dependence of R_{EX} on the pulsing rate ν_{cp} in a standard CPMG-echo sequence is related to forward (k_1) and reverse (k_{-1}) rate constants for exchange between the two "sites", their relative equilibrium populations p_A and p_B, and the chemical shift difference $\Delta\omega$. Relaxation dispersion thus potentially provides kinetic, thermodynamic, and structural information about protein states that are not visible in the NMR spectra.[41] Representative dispersion curves are shown in Figure 4. The dispersion data were fit to the two-site fast-exchange equation (eq 2), which is valid if $k_{EX} > \Delta\omega$.[24] Equation 2 provides k_{EX} from a single dispersion curve, but does not allow for unambiguous determination of $\Delta\omega$ or p_A, and thus not k_1 and k_{-1} (eqs 3a, 3b). We therefore sought to determine $\Delta\omega$ separately. To this end, we lowered k_{EX} by decreasing the sample temperature and expected a maximum in R_{EX} when the condition $k_{EX} = \Delta\omega$ was met.[24] Figure 4 shows the maximum in R_{EX} in each anhydrous solvent. At this particular temperature, k_{EX} was calculated from a dispersion curve. and its value was taken as $\Delta\omega$. For SC extracted in isooctane, $\Delta\omega = 455\ s^{-1}$, and in THF $\Delta\omega = 190\ s^{-1}$.

$$R_2 = R_2(\upsilon_{CP} \rightarrow \infty) + R_{EX} \tag{1}$$

$$R_{EX}(\nu_{CP}) = \left(\frac{p_A p_B \Delta\omega^2}{k_{EX}}\right)\left(1 - \frac{2\nu_{CP}\tanh\left(\frac{k_{EX}}{2\nu_{CP}}\right)}{k_{EX}}\right) \tag{2}$$

$$k_{EX} = k_1 + k_{-1} \tag{3a}$$

$$p_A k_{-1} = p_B k_1 \tag{3b}$$

$$\alpha = \left(\frac{B_0^2 + B_0^1}{B_0^2 - B_0^1}\right)\left(\frac{R_{EX}^2 - R_{EX}^1}{R_{EX}^2 + R_{EX}^1}\right),\ \alpha > 1 \text{ if } k_{EX} > \Delta\omega \tag{4}$$

The scaling parameter $\alpha = 1.25$ was determined at 282 and 376 MHz using eq 4, validating use of the fast exchange equation.[42]

Active-Site Dielectric Constant from Chemical Shift. The chemical shift of 4FBS-SC was empirically converted to a dielectric constant ε (eq 5) by recording the ^{19}F chemical shift of the aromatic resonance of free 4FBSF in solvents of known dielectric constant. Over the range $2 < \varepsilon < 20$, the relationship was linear (Figure S2). When 4FBS was attached to the active site, this empirical relation was used to calculate the active-site dielectric constant ε_{as}.

$$\varepsilon = \frac{(\delta - \delta_{CFCl_3}) + 98.7(\pm 0.4)}{-0.36(\pm 0.02)} \tag{5}$$

The Kirkwood model predicts a reduction in the free energy of a zwitterionic dipole embedded in a solvent when the dielectric factor q of the solvent is increased.[30] In subtilisin catalysis, the APEE-active-site transition state is the charged dipole with radius $r_{ES^{\mp}}$, and the surrounding enzyme/solvent is a continuum with dielectric constant ε_{as}. As applied here, the model predicts transition state free energies $\Delta G^{\ddagger}$ to be dependent on q through the transition state dipole moment $\mu_{ES^{\mp}}$.[31] The difference in free energy $\Delta\Delta G^{\ddagger}$ between enzyme preparations was calculated from the catalytic efficiency k_{cat}/K_M and referenced to the $a_w = 0$ preparation in each solvent (eqs 6−8).

(36) Gerig, J. T.; Hammond, S. J. *J. Am. Chem. Soc.* **1984**, *106*, 8244–8251.
(37) Lipari, G.; Szabo, A. *J. Am. Chem. Soc.* **1982**, *104*, 4546–4559.
(38) Woessner, D. *J. Chem. Phys.* **1962**, *36*, 1–4.
(39) Mulder, F. A.; Mittermaier, A.; Hon, B.; Dahlquist, F. W.; Kay, L. E. *Nat. Struct. Biol.* **2001**, *8*, 932–5.
(40) McElheny, D.; Schnell, J. R.; Lansing, J. C.; Dyson, H. J.; Wright, P. E. *Proc. Natl. Acad. Sci. U.S.A.* **2005**, *102*, 5032–7.
(41) Carver, J.; Richards, R. *J. Magn. Reson.* **1972**, *6*, 89–105.
(42) Millet, O.; Loria, J. P.; Kroenke, C. D.; Pons, M.; Palmer, A. G. *J. Am. Chem. Soc.* **2000**, *122*, 2867–2877.

$$\Delta\Delta G^{\mp} = -RT\ln\left[\frac{(k_{cat}/K_M)}{(k_{cat}/K_M)_{a_w=0}}\right] \quad (6)$$

$$\Delta\Delta G^{\mp} = -N_A\left(\frac{\mu^2}{r^3}\right)\Delta q \quad (7)$$

$$\Delta q = \left(\frac{\varepsilon_{as}-1}{2\varepsilon_{as}+1}\right) - \left(\frac{\varepsilon_{as}-1}{2\varepsilon_{as}+1}\right)_{a_w=0} \quad (8)$$

Experimental Section

Extraction of Subtilisin into Organic Solvents. The extraction of enzymes and SC (Sigma) in particular into organic solvents containing the surfactant Aerosol OT (AOT) has been described previously.[43−45] The efficiency of SC extraction into isooctane containing 2 mM AOT from aqueous buffer ranged from 20% to 30%. The organic-soluble enzyme was concentrated by complete evaporation of isooctane and redissolved in the appropriate solvent to 1−13 mg/mL depending on the application.

Transesterification of N-Ac-Phe-Ethyl Ester. Specific thermodynamic activities of water in solutions containing the organic-soluble enzyme and reaction reagents were set using hydrated salt pairs and salt-saturated aqueous solutions.[46] The organic solvents (either pure or containing 1.7 M 1-PrOH) were pre-equilibrated with hydrated salt pairs (NaI 2/0, a_w 0.07; Na_2HPO_4 2/0, a_w 0.16; NaAc 3/0, a_w 0.35; or Na_2HPO_4 7/2, a_w 0.61) and stored for many months. Extracted SC and the transesterification reagents (i.e., N−Ac−Phe−ethyl ester (APEE) and nonadecane) were dissolved separately at twice (2×) the reaction concentrations in the pure and 1-PrOH-containing solvents, respectively. Equilibration to the final desired a_w was achieved by placing open vials (2 mL) of these solutions in a sealed vessel containing the saturated salt solution appropriate for the desired a_w. The solutions were allowed to equilibrate at room temperature for 24 (isooctane) or 2 h (THF). Karl Fischer titration was used to determine the water content of each preparation to ensure that the 24 and 2 h periods were sufficiently long for the water concentration to reach equilibrium in each solvent.

Transesterification of 2−50 mM (isooctane solvent) and 20−200 mM (THF solvent) of APEE was performed with 0.85 M 1-PrOH and 2−4 mg/mL extracted SC at 30 °C and 180 rpm. Equal volumes of the extracted SC and reagent solutions equilibrated to a given a_w were mixed so that all components were diluted 2-fold. The following procedure was used to determine that a_w did not change upon mixing of the two pre-equilibrated solutions. Solutions of 0.85 and 1.7 M 1-PrOH were equilibrated to a given a_w, and the water contents were determined by Karl Fischer titration. The 1.7 M 1-PrOH isooctane solution contained twice as much water as the 0.85 M 1-PrOH solution, indicating that diluting the water concentration 2-fold upon mixing of the original SC and reagent solutions did not alter a_w. In THF, the presence of 1-PrOH at either 0.85 or 1.7 M did not significantly affect the measured water concentration in the range of a_w values tested, indicating that mixing of the reagents in THF did not alter a_w.

Aliquots of 200 μL were removed periodically for up to 6 h and heated rapidly to 90 °C to denature and precipitate the SC. Reaction progress was monitored by formation of *N*-Ac-Phe-propyl ester (APPE) using gas chromatography, as described previously.[9] Initial rates of APPE formation at each APEE concentration were fit to the Michaelis−Menten equation to determine the catalytic constants k_{cat}^{app} and K_M^{app}.

The concentration of active sites in each preparation was calculated using the method of Wangikar et al.[47] This procedure determines the fraction of active sites titratable with the protease inhibitor PMSF in a given solvent preparation, relative to the concentration of active sites in buffer. The fraction of titratable active sites for aqueous SC was assumed to be 63% of total protein content.[47] The fraction of the 63% that was active in THF preparations ranged from 3% to 25%, and in isooctane from 75% to 85%.

Preparation of 4FBS-Subtilisin. The synthesis of the SC inhibitor, 4-fluoro-benzenesulfonyl fluoride (4FBSF), has been described previously.[48] SC was dissolved to 10 mg/mL in 20 mM Bis-Tris propane buffer containing 2 mM $CaCl_2$, pH 7.8. A 20-fold molar excess solution of 4FBSF in acetone was added to 5% volume, and the mixture was gently stirred at 30 °C for 2 h. SC was checked for reactivity against Suc-Ala-Ala-Pro-Phe-nitroanalide (SAAPFpNA) before and after 4FBSF addition, and the enzyme was found to be >95% inactivated. Excess 4FBSF was then removed by filter centrifugation (Millipore Amicon 30 kDa MWCO), and the retentate was diluted in aqueous buffer. The inhibited enzyme was extracted into organic solvent, concentrated by evaporation, and equilibrated to the desired a_w.

^{19}F NMR Spectroscopy. ^{19}F NMR spectra were collected at 1.5, 7.1, and 9.4 T on Tecmag LapNMR, Tecmag Apollo, and Bruker Avance spectrometers, respectively, without proton decoupling. Extracted SC in NMR samples was between 0.2 and 0.5 mM (5−12 mg/mL) in 5 mm o.d. tubes for 9.4 T experiments, and in 10 mm o.d. tubes for 7.1 and 1.5 T experiments. R_1 was determined from the inversion recovery method, and R_2 was determined using the CPMG-echo pulse sequence with a pulse separation of 50 μs. Relaxation dispersion curves (Figure 4) were obtained at temperatures 0−40 °C at 9.4 T, and at 22 °C at 7.1 T. The duration of the 180 pulse was calibrated for each temperature and static field and was 14−18 μs. Typically, 8k (9.4 T) or 64k (7.1 T) scans were taken at each pulsing rate, with 0.8 s delay between scans. The relaxation dispersion curves were fit to eq 2 using the program Mathematica, with error ranges reported.

{^{1}H}^{19}F NOEs were determined at 7.1 T. Subtraction of spectra accumulated with and without ^{1}H irradiation during the preacquisition period was used to calculate the NOE factor. Typical ^{1}H saturation times were 200 ms.

The empirical relation of ^{19}F chemical shift and solvent dielectric constant was generated by recording the chemical shift of the aromatic resonance of 4FBSF with respect to trifluoroacetic acid at 9.4 T. The 4FBSF was dissolved at 0.01−0.5 mM in each solvent and desiccated for 24 h to remove all water. The solution was transferred to an NMR tube with a small capillary containing TFA. The solvent dielectric constants were taken from the CRC Handbook.

Circular Dichroism. Far-UV circular dichroism spectra were obtained on an Aviv 410 spectrometer following a protocol published previously.[21] SC concentrations were 0.2−0.3 mg/mL. Molar ellipticity at 222 nm was calculated using a mean residue weight of 100.

Dynamic Light Scattering. Dynamic light scattering experiments on organic-soluble SC followed a protocol published previously.[43] The correlation time for protein tumbling τ_c was determined from the hydrodynamic radius using the Stokes equation for spheres. The viscosities of solvent−AOT mixtures were calculated from empirical equations[49] and varied <3% from the pure solvent viscosity.

Molecular Modeling. The active site of 4BS-subtilisin was modeled using the Maestro program. SC coordinates (PDB ID 1SBC[50]) were loaded into the program, and 4-FBS was built into the active site at Ser221 in various orientations. 4FBS and active-

(43) Akbar, U.; Aschenbrenner, C. D.; Harper, M. R.; Johnson, H. R.; Dordick, J. S.; Clark, D. S. *Biotechnol. Bioeng.* **2007**, *96*, 1030–9.
(44) Adachi, M.; Harada, M. *J. Phys. Chem.* **1993**, *97*, 3631–3640.
(45) Paradkar, V. M.; Dordick, J. S. *Biotechnol. Bioeng.* **1994**, *43*, 529–540.
(46) Hutcheon, G. A.; Halling, P. J.; Moore, B. D. *Lipases, Part B* **1997**, *286*, 465–472.
(47) Wangikar, P. P.; Carmichael, D.; Clark, D. S.; Dordick, J. S. *Biotechnol. Bioeng.* **1996**, *50*, 329–335.
(48) Gerig, J. T.; Roe, D. C. *J. Am. Chem. Soc.* **1974**, *96*, 233–8.
(49) Gomez-Diaz, D.; Mejuto, J. C.; Navaza, J. M. *J. Chem. Eng. Data* **2006**, *51*, 409–411.

site protein atoms were then allowed to relax to an energetic minimum. The lowest energy minimum structure is shown in Figure 3.

Acknowledgment. This work was supported by the National Science Foundation (BES-0228145) and the National Institutes of Health (GM66712). We are grateful to Rudi Nunlist for assistance with the ^{19}F NMR experiments.

Supporting Information Available: Coordinates for the minimized 4FBS-SC structure as a PDB file at the following Internet address: http://india.cchem.berkeley.edu/~reimer/hudson/1SBC4BS.pdb. Circular dichroism and nuclear Overhauser effect results on the global and active site structure of organic-soluble SC in isooctane and THF. Relation between ^{19}F chemical shift of 4FBSF and solvent dielectric constant. This material is available free of charge via the Internet at http://pubs.acs.org.

JA806996Q

(50) Neidhart, D. J.; Petsko, G. A. *Protein Eng.* **1988**, *2*, 271–6.
(51) Xu, Z. F.; Affleck, R.; Wangikar, P. P.; Suzawa, V.; Dordick, J. S.; Clark, D. S. *Biotechnol. Bioeng.* **1994**, *43*, 515–520.